ACS OMEGA

Open Access

http://pubs.acs.org/journal/acsodf

Article

Metabolic Engineering of *Escherichia coli* for Efficient Production of Pseudouridine

Min Zhou,* Ruyu Tang, Liyuan Wei, Jidong Wang, and Huan Qi

Cite This: *ACS Omega* 2023, 8, 36386−36392

Read Online

ACCESS | Metrics & More | Article Recommendations | Supporting Information

ABSTRACT: Pseudouridine-incorporated mRNA vaccines can enhance protein expression and reduce immunogenicity, leading to a high demand for pseudouridine to be used in mRNA drug production. To achieve the low-cost production of pseudouridine, *Escherichia coli* was systematically modified to utilize inexpensive raw materials to efficiently produce pseudouridine. First, in the pyrimidine biosynthesis pathway, genes related to the precursor competing pathway and the negative regulator were deleted, which increased pseudouridine production. Second, two critical genes, pseudouridine-5′-phosphate glycosidase (*psuG*) and phosphatase genes from different bacteria, were screened and employed in various genetic constructs, and the pseudouridine yield of the optical strain increased to 599 mg/L. The accumulation of pseudouridine was further increased by the deletion of pseudouridine catabolism-related genes. Ultimately, the pseudouridine titer in a 5 L bioreactor reached 7.9 g/L, and the yield of pseudouridine on glucose was 0.15 g/g. Overall, a cell factory producing pseudouridine was successfully constructed and showed potential for industrial production.

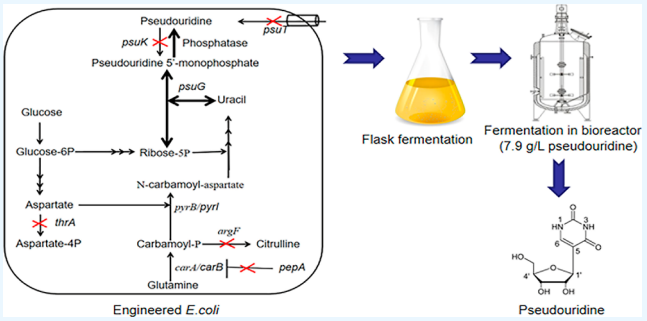

INTRODUCTION

Pseudouridine (Ψ) was isolated from yeast more than 50 years ago[1] and, as 5-ribosyl uracil, was considered the fifth nucleoside to be identified. It is the most abundant natural *C*-nucleoside and has been found in tRNA, small nuclear RNA, nucleolar RNA, and even in the coding regions of mRNA.[2] Pseudouridine exhibits important biological functions, impacts various aspects of RNA biology, and confers distinct structural and functional properties.[3] Pseudouridine modifications can increase the stability of mRNA,[4] enhance protein expression and reduce immunogenicity,[5,6] and play critical roles in increasing the efficiency of mRNA vaccines against COVID-19.[7]

COVID-19 mRNA vaccines have led to a high demand for pseudouridine. As of 19 April 2023, 2328 clinical trial registrations were shown in the Clinical Trials Database[8] when the keyword "mRNA" was entered as the search term, which suggested that many new mRNA drugs will be approved and lead to a large demand for pseudouridine in the future. To date, there have been three approaches to produce pseudouridine. The first approach involves a total chemical synthesis. Several synthetic routes have been successfully developed, but multiple steps are needed; moreover, the yields are low, and the costs are high.[9,10] The second approach involves natural biosynthesis. In nature, pseudouridine is synthesized by pseudouridine synthase-catalyzed posttranslational isomerization of RNA uridine.[11] Due to the low pseudouridine content in RNA,[12] large-scale production of pseudouridine by hydrolyzing RNA is unfeasible. The third approach involves enzymatic synthesis. Pseudouridine-metabolizing genes were identified in *Escherichia coli*. Pseudouridine is first phosphorylated by pseudouridine kinase (*psuK*) to be pseudouridine 5′-phosphate, and then pseudouridine 5′-phosphate is hydrolyzed by PsuG into uracil and ribose 5′-phosphate.[13] Meanwhile, PsuG has reversible catalytic activity, which can catalyze uracil and ribose 5′-phosphate to synthesize pseudouridine 5′-phosphate. Then, pseudouridine 5′-phosphate is dephosphorylated by phosphatase to generate pseudouridine.[13,14] This reverse reaction was used for the enzymatic synthesis of pseudouridine. The first report of the enzymatic synthesis of pseudouridine was published in 2008. Uracil and ribose 5′-phosphate were catalyzed by pseudouridine 5′-phosphate glycosidase (psuG) to synthesize pseudouridine 5′-phosphate, and pseudouridine-5′-phosphate was dephosphorylated by alkaline phosphatase (phoA) to obtain pseudouridine (Figure 1A).[13] A semi-enzymatic synthesis approach was developed for the synthesis of pseudouridine.[15] In this approach, the substrate ribose 5′-phosphate was

Received: July 19, 2023
Accepted: September 6, 2023
Published: September 23, 2023

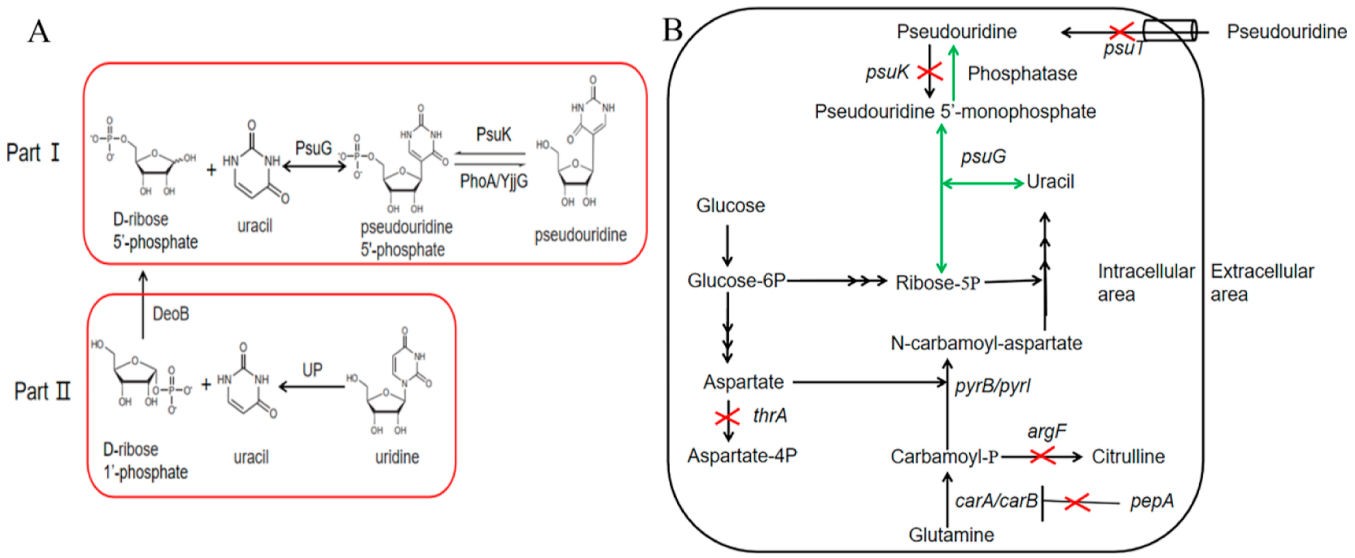

Figure 1. Biosynthesis of pseudouridine. (A) Enzymatic synthesis of pseudouridine. (B) Scheme for the construction of the pseudouridine production strain. Single arrows represent one-step biosynthesis, triple arrows represent multistep biosynthesis, green arrows indicate gene overexpression, and "X" indicates deletion of the corresponding gene.

hydrolyzed from adenosine 5′-monophosphate. Recently, a robust biocatalytic process technology was established. *yjjG* was identified as a ΨMP-specific phosphatase and was used to replace gene phoA to synthesize pseudouridine, as shown in Figure 1A (Part I). Multienzyme cascade reactions transformed uridine into pseudouridine (Figure 1A) with a productivity of 40 g/L/h, exhibiting high promise for use in production.[14]

Because the starting materials used in the enzymatic process have relatively high costs, pseudouridine production by fermentation from cheap glucose is an attractive alternative. In recent years, *E. coli* has been widely used to construct cell factories for natural product biosynthesis. In general, the host strain used to build cell factory needs to meet the following requirements: a clear genetic background, highly efficient genetic manipulation methods, fast growth, a sufficient supply of metabolic precursors, the ability to utilize cheap raw materials, and an efficient fermentation process. *E. coli* fully meets these requirements.[16] Furthermore, *E. coli* has a highly efficient production of pyrimidine nucleosides and has been used to produce uridine and cytidine from glucose via fermentation.[17,18] Therefore, *E. coli* was chosen to be genetically engineered to produce pseudouridine by fermentation. Several strategies were used to engineer *E. coli* for the efficient production of pseudouridine in this study (Figure 1B). First, we deleted the genes related to the precursor competing pathway and the negative regulator. Second, we screened and overexpressed the efficient *psuG* (formerly known as *yeiN*) and phosphatase genes. Third, we deleted the pseudouridine catabolism-related genes. Finally, the optimal strain produced 7.9 g/L of pseudouridine in a 5 L bioreactor by fed-batch fermentation.

RESULTS AND DISCUSSION

Engineering of the Pyrimidine Biosynthesis Pathway to Increase Pseudouridine Production. The starting substrates used for pseudouridine enzymatic synthesis existed in *E. coli* MG1665.[13,17] Nevertheless, no pseudouridine was detected by HPLC in the shake flask fermentation broth of *E. coli* MG1655. When *phoA* and *EcpsuG* (from MG1665) were overexpressed in MG1665, after flask fermentation, the yielding strain MG1655(pET30phoAEcpsuG) could accumulate pseudouridine. Pseudouridine was isolated as a white amorphous powder. Its molecular formula was determined to be $C_9H_{12}N_2O_6$ on the basis of HRESIMS at m/z 267.0586 $[M + Na]^+$ (calcd 267.0593 for $C_9H_{12}N_2O_6Na$) (Figure S1), indicating 5 degrees of unsaturation. The ^{1}H nuclear magnetic resonance (NMR) spectrum (Figure S2) showed a downfield singlet proton at δ_H 7.59 (1H, s), four oxygen-bearing methine protons at δ_H 4.60 (1H, d, J = 5.5 Hz), 4.22 (1H, t, J = 5.4 Hz), 4.07 (1H, t, J = 5.4 Hz), 3.95 (1H, m, H-4′) and two oxygen-bearing methylene protons at δ_H 3.77 (1H, dd, J = 12.5, 3.2 Hz), 3.65 (1H, dd, J = 12.5, 4.8 Hz). Its ^{13}C NMR spectrum (Figure S3) displayed 9 carbon resonances, including two amide carbonyl carbons at δ_C 165.34 and 152.85, one sp^2 methine at δ_C 141.55, one sp^2 quaternary carbon at δ_C 110.52, four oxygenated methines at δ_C 83.39, 79.20, 73.38, 70.85, and one oxygenated methylene at δ_C 61.53. The structure was elucidated as pseudouridine by comparing the ^{1}H and ^{13}C NMR data of pseudouridine with the NMR data reported by Pfeiffer et al.[14] The pseudouridine yield of MG1655-(pET30phoAEcpsuG) was 29.5 mg/L (Figure 2). Among the pseudouridine biosynthetic precursors, uracil accumulated to 289 mg/L (Figure 2), while ΨMP and uridine were not significantly accumulated (Figure S4).

To increase the pseudouridine production, the pyrimidine biosynthesis pathway was engineered (Figure 1). *thrA*[17] and *argF*[19] were successively knocked out to block the precursor competing pathway. Subsequently, the negative regulator *pepA*[20] was deleted to enhance pyrimidine biosynthesis, which yielded strain PSU3. Next, plasmid pET30phoAECpsuG was transformed into PSU3, yielding strain PSU3-(pET30phoAECpsuG). The pseudouridine yield of PSU3-(pET30phoAECpsuG) increased to 102.7 mg/L, which is about 3.5-fold that of MG1655(pET30phoAEcpsuG), and the yield of uracil increased to 793 mg/L (Figure 2), which illustrated that pyrimidine biosynthesis pathway optimization was effective in improving pseudouridine production. How-

https://doi.org/10.1021/acsomega.3c05219
ACS Omega 2023, 8, 36386−36392

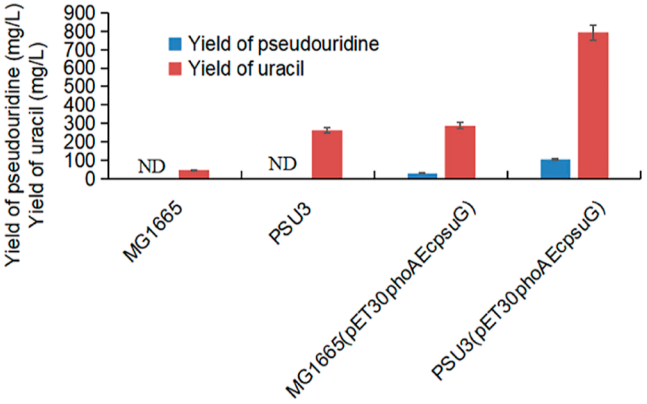

Figure 2. Enhancing the production of pseudouridine by engineering the pyrimidine biosynthesis pathway. ND: not detectable.

ever, there was a high accumulation of uracil, which suggested that pseudouridine synthesis reactions from uracil were rate-limiting steps.

Screening the Phosphatase Gene for Efficient Pseudouridine Production. The ΨMP synthesis reaction involving ΨMP glycosidase was favored for pseudouridine production and was promoted by ΨMP dephosphorylation.[15,21] Therefore, the ΨMP glycosidase and phosphatase genes were the focus of this study. First, the phosphatase genes were screened to determine the most suitable genes for pseudouridine production. SDT1, YKL033W-A, and PHM8 from *Saccharomyces cerevisiae* have been reported to show ΨMP dephosphorylation activity.[22] *pumD* was predicted to be involved in pseudouridine biosynthesis and function as a phosphatase,[23] so *pumD* was selected to test whether it has ΨMP dephosphorylation activity. Recently, YjjG in *E. coli* was discovered to be a ΨMP-specific phosphatase.[14] Then, the five genes, namely, *SDT1*, *YKL033W-A*, *PHM8*, *pumD*, and *yjjG* were chosen and overexpressed with *EcpsuG* in PSU3, which yielded strains PSU3(pET30SDT1EcpsuG), PSU3(pET30YKL033WEcpsuG), PSU3(pET30PHM8EcpsuG), PSU3(pET30pumDEcpsuG), and PSU3(pET30yjjGEcpsuG), respectively. All five genes led to improved pseudouridine yields after fermentation in shake flasks, which were approximately 3-fold higher than those produced with *phoA* (Figure 3A). Among these genes, *yjjG* was the most efficient for pseudouridine production, and the yield of PSU3(pET30yjjGEcpsuG) was the highest, reaching 403 mg/L (Figure 3A), which is about 3.9-fold that of PSU3(pET30phoAEcpsuG). The ratio of uracil to pseudouridine in the fermentation broth of PSU3(pET30phoAEcpsuG) was 8, and the ratio of PSU3(pET30yjjGEcpsuG) decreased to 1.5 (Figure 3A). The pseudouridine yield of PSU3(pET30pumDEcpsuG) was 393 mg/L, which was slightly lower than that of PSU3(pET30yjjGEcpsuG) but had no significant differences. The other three genes, *SDT1*, *YKL033W-A*, *PHM8*, produced less pseudouridine and more uracil than those produced with *yjjG* (Figure 3A). These results suggested that *yjjG* had a higher dephosphorylation activity against ΨMP and promoted pseudouridine biosynthesis.

Protein electrophoresis (Figure S5) analysis of the supernatants showed that all of the phosphatases tested were correctly expressed, although there were some differences in expression levels. Enzymatic assays revealed that PhoA had the lowest activity among the five phosphatases, and *yjjG*[14] had the highest activity and substrate affinity (Table S1). Therefore, *yjjG* was chosen for subsequent experiments.

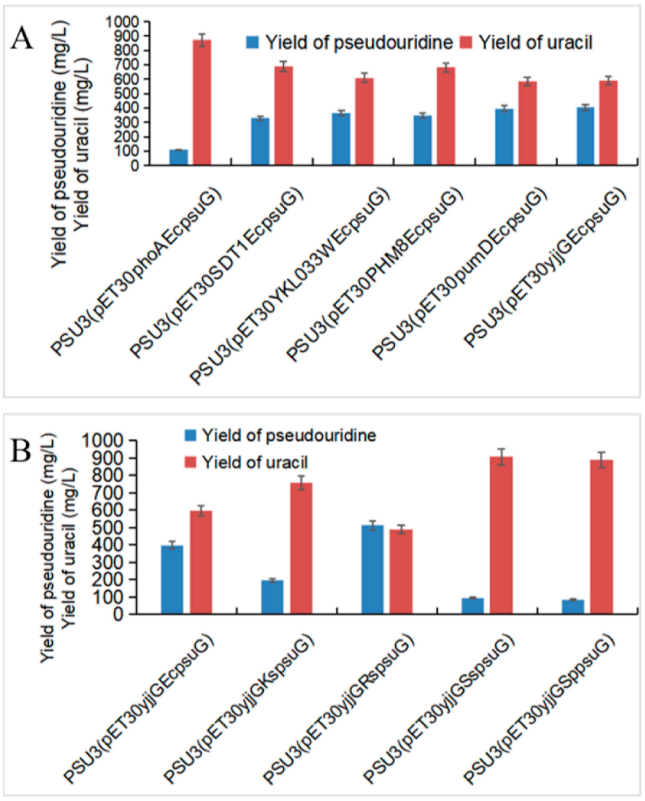

Figure 3. Screening phosphatase and *psuG* genes optimal for pseudouridine production. (A) Production of pseudouridine with different phosphatase genes. (B) Production of pseudouridine with different *psuG* genes.

It is worth noting that all of these phosphatases belong to the haloacid dehalogenase protein family,[14,22,23] which suggests that haloacid dehalogenases are potential sources for screening more efficient phosphatases for use in pseudouridine production. Haloacid dehalogenase family phosphatases detoxify ΨTP and ΨMP in *S. cerevisiae*,[22] and genome analysis revealed that Group I C-glycosynthases usually coexist with a haloacid dehalogenase family phosphatase gene located in the vicinity of the C-glycosynthase gene,[24] which may support the speculation that haloacid dehalogenases are candidates for screening more efficient phosphatases against ΨMP.

Screening the ΨMP Glycosidase Gene for Efficient Pseudouridine Production. *psuG* has bidirectional catalysis activity; it can hydrolyze ΨMP to uracil and ribose 5-phosphate, and it can also catalyze the reverse reaction to synthesize pseudouridine and other xenobiotic nucleic acids.[15,21] It is widely present in the genomes of prokaryotes.[24] In this study, *EcpsuG* and four other *psuG* genes from different sources were tested: *KspsuG* (from *Klebsiella spallanzanii*), *RspsuG* (from *Rhizobium* sp. CF142), *SspsuG* (from *Saccharopolyspora spinosa*), and *SppsuG* (from *Streptomyces platensis*). These genes came from bacteria belonging to different genera and had different genetic distances from *EcpsuG* (Figure S6). The plasmids carrying the four aforementioned codon-optimized *psuG* genes co-overexpressed with *yjjG* were transformed into PSU3, yielding strains PSU3(pET30yjjGKspsuG), PSU3(pET30yjjGRspsuG), PSU3(pET30yjjGSspsuG), and PSU3(pET30yjjGSppsuG). Com-

https://doi.org/10.1021/acsomega.3c05219
ACS Omega 2023, 8, 36386−36392

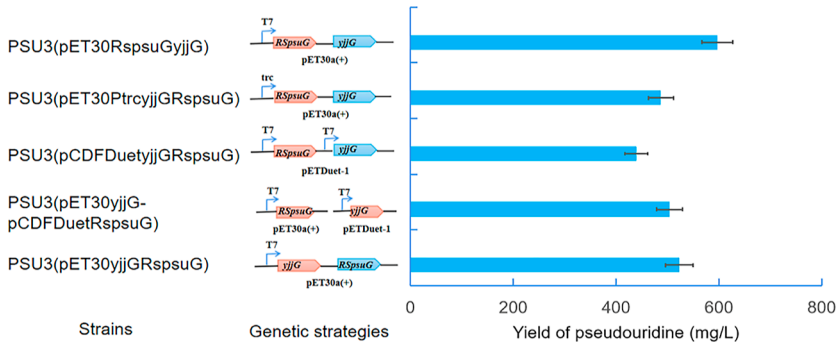

Figure 4. Production of pseudouridine was achieved with different genetic strategies.

pared with that of PSU3(pET30yjjGEcpsuG), the titer of pseudouridine from PSU3(pET30yjjGRspsuG) was increased by 27% and reached 511 mg/L, which was the highest among all of the aforementioned strains (Figure 3B). The ratio of uracil to pseudouridine in the fermentation broth of PSU3-(pET30yjjGRspsuG) decreased to 0.96 (Figure 3B), which might suggest that RspsuG was more prone to reverse reaction to synthesize ΨMP compared with other psuG enzymes. *KspsuG* produced 196.5 mg/L pseudouridine, which was half of those produced with *RspsuG*, and *SspsuG* only produced 96.2 mg/L pseudouridine (Figure 3B). Pseudouridine was detected in the fermentation broth of *S. platensis*,[25] but *psuG* from *S. platensis* was not efficient for pseudouridine production, and the yield of PSU3(pET30yjjGSppsuG) was only 83.7 mg/L (Figure 3B).

Protein electrophoresis (Figure S7) analysis of the supernatants showed that all of the PsuG proteins tested were correctly expressed. Enzymatic assays revealed that RspsuG had the most activity and substrate affinity compared to the others, and it was 6-fold more efficient and showed 1.57-fold more substrate affinity than EcpsuG (Table S2).

Fine-Tuning of Gene Expression. Various factors, such as plasmid copy number, promoter strength, gene copy number, and the order of genes, can affect the yield of natural compounds in *E. coli*.[26,27] To further improve the yield of pseudouridine, five recombinant *E. coli* strains were constructed according to different genetic strategies (Figure 4). There were significant differences in the pseudouridine yield under different genetic strategies. PSU3(pET30RspsuGyjjG) exhibited the highest yield, reaching 599 mg/L (Figure 4). The only difference between PSU3(pET30RspsuGyjjG) and PSU3-(pET30yjjGRspsuG) was the cloning order of *yjjG* and *RspsuG*; however, the yield ofPSU3(pET30yjjGRspsuG) was lower than that of PSU3(pET30RspsuGyjjG). When the T7 promoter of pET30RspsuGyjjG was replaced by the trc promoter, the yield of PSU3(pET30PtrcyjjGRspsuG) decreased. When *yjjG* and *RspsuG* were cloned in pCDFDuet-1 under the individual T7 promoter, although the copy number increased, the yield of PSU3(pCDFDuetyjjGRspsuG) was the lowest (Figure 4), which might be due to the increased metabolic burden with the increased copy number.

Knockout of Pseudouridine Catabolism-Related Genes. The involvement of *psuK* has been identified in pseudouridine metabolism in *E. coli* UTI89 and specifically phosphorylates pseudouridine to yield pseudouridine 5′-phosphate. *psuT* was predicted to function in pseudouridine uptake in cooperation with *psuK* and *psuG* to metabolize extracellular pseudouridine.[13,28] Based on their functions, the knockout of *psuK* and *psuT* was expected to contribute to pseudouridine accumulation. *psuK* and *psuT* were successively deleted in PSU3, yielding PSU4 and PSU5s, respectively. Plasmid pET30RspsuGyjjG, which exhibited the most efficient pseudouridine production, was transformed into PSU4 and PSU5, yielding strains PSU4(pET30RspsuGyjjG) and PSU5-(pET30RspsuGyjjG), respectively. The deletion of *psuK* exerted no positive effect on pseudouridine production (Figure 5). After deleting *psuT*, the yield of PSU5(pET30RspsuGyjjG)

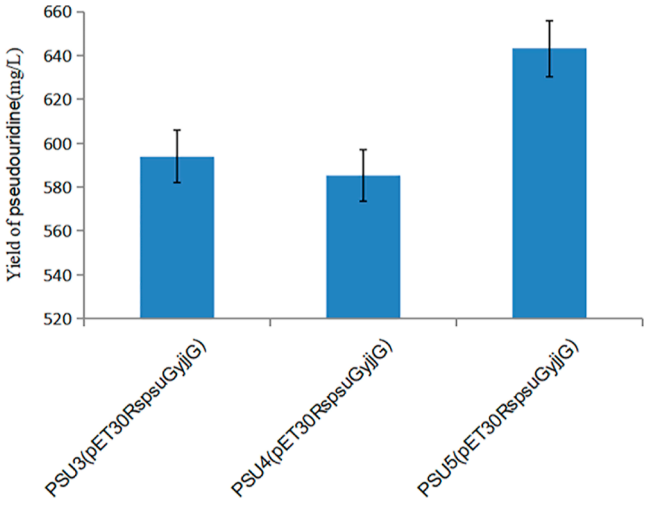

Figure 5. Effects of deleted pseudouridine catabolism-related Genes on pseudouridine accumulation.

increased by 7%, reaching 642 mg/L (Figure 5). The fermentation results of the *psuT* mutant suggested that blocking the pseudouridine uptake was conducive to the accumulation of pseudouridine.

Fed-Batch Fermentation of Pseudouridine in a 5 L Bioreactor. The strain PSU5(pET30RspsuGyjjG), which exhibited the highest yield of pseudouridine in shake flasks, was used to explore the production potential of a fed-batch fermentation strategy under the indicated cultivation conditions. As shown in Figure 6, during the growth stage, the 10 g/L glucose concentration initially used was almost exhausted after 4 h, and the glucose was then fed at the appropriate rate. In the initial 8 h, the cells grew exponentially, but no product accumulated. Isopropyl-*β*-D-thiogalactopyranoside (IPTG) was added to the medium after 8 h of cultivation, and the fermentation temperature was decreased to 30 °C, which was optimal for ΨMP glycosidase synthesis.[15] Then, pseudouridine began to accumulate. The cell concentration reached a maximum at 32 h, after which the OD_{600} value began to

https://doi.org/10.1021/acsomega.3c05219
ACS Omega 2023, 8, 36386−36392

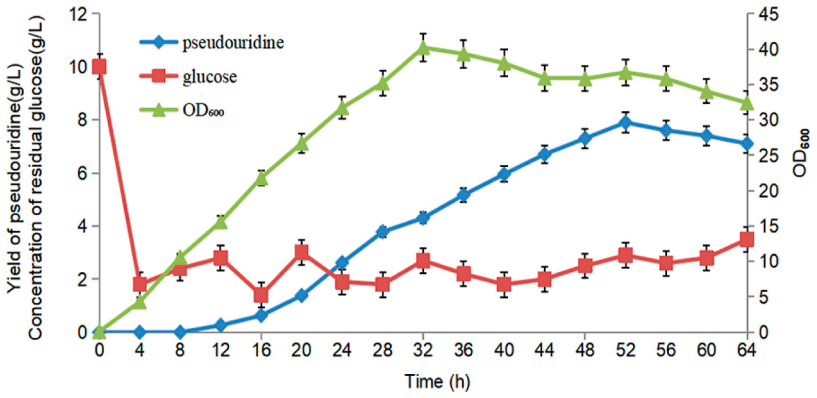

Figure 6. Fed-batch fermentation profiles of PSU5(pET30RspsuGyjjG) in a 5 L bioreactor.

decrease steadily, but pseudouridine continued to accumulate, exhibiting a cell-growth-independent production profile. At 52 h, the final pseudouridine titer reached 7.9 g/L, and the yield of pseudouridine on glucose was 0.15 g/g.

CONCLUSIONS

In this study, a cell factory producing pseudouridine was successfully constructed. The deletion of *argF*, *thrA*, and *pepA*, which are involved in pseudouridine precursor biosynthesis, increased pseudouridine production. *psuG* is from *Rhizobium* sp. CF142 and *yjjG* from *E. coli* constituted the most efficient combination for pseudouridine biosynthesis. The deletion of *psuT* further increased the yield of pseudouridine. Ultimately, the yield of pseudouridine reached 7.9 g/L with a yield of 0.15 g/g of glucose in a 5 L bioreactor via fed-batch fermentation. To our knowledge, this is the first report of engineered *E. coli* producing pseudouridine. This study provides a foundation for low-cost industrial production of pseudouridine via microbial fermentation.

MATERIALS AND METHODS

Bacterial Strains and Culture Conditions. The strains used in this study are listed in Table S1. *E. coli* DH5α was used as the cloning host. *E. coli* MG1665 was used in genome-editing experiments and as the host strain for pseudouridine production. *E. coli* cells were cultivated at 37 °C in Luria–Bertani (LB) medium for clone construction experiments and seed preparation. Kanamycin (50 mg/L), ampicillin (50 mg/L), and spectinomycin (50 mg/L) were added as needed.

The fermentation medium (20 g of glucose, 10 g of yeast extract, 6 g of KH_2PO_4, 16.4 g of K_2HPO_4, 5 g of $(NH_4)_2SO_4$, 1.1 g of citric acid, 1 g of $MgSO_4$, 15 mg of $MnSO_4$, and 2 mg of V_{B1} in 1000 mL of water) was used for shake flask fermentation. IPTG was added to the medium at a final concentration of 0.1 mM when the OD_{600} reached 0.6, and the temperature was adjusted to 30 °C.

Fed-batch fermentation was initiated with 10 g/L glucose. The other components in the medium were the same as those in the flask fermentation medium. After 8 h of culture, IPTG was added to the medium to a final concentration of 0.1 mM, and the temperature was adjusted to 30 °C. The pH was maintained at 7.0 via the automated addition of a 25% (v/v) NH_4OH solution. The dissolved oxygen saturation level was controlled to be greater than 25% by adjusting the aeration and agitation rates. The concentration of glucose was maintained at less than 5 g/L by feeding 600 g/L of glucose at the appropriate rate.

Construction of Recombinant Plasmids. The plasmids used in this study are listed in Table S3. The primers used for gene cloning are given in Table S4. EPSUax Universal CloneMix (Tolobio) was used for plasmid construction. The plasmid pET-30a (+) was used as a cloning vector and for pseudouridine production. *phoA* DNA fragments originating from *E. coli* MG1655 were amplified from its genomic DNA by PCR and ligated with linearized pET-30a (+) that had been digested by NdeI, resulting in pET30phoA. The *EcsuG* DNA fragments (from *E. coli* MG1655) were amplified by PCR and ligated to linearized pET-30phoA that had been digested by EcoRV, resulting in pET-30phoAECpsuG. The RBS sequence (aaaggaggatatacat) was inserted in front of the *psuG* start codon. *SDT1*, *YKL033W-A*, and *PHM8*, originating from *S. cerevisiae*, *pumD* originating from *Streptomyces* sp. ID38640 and *yjjG* were cloned into pET-30a (+) with *EcpsuG* using a similar method, yielding plasmids pET30SDT1ECpsuG, pET30YKL033WECpsuG, pET30PHM8ECpsuG, pET30pumDECpsuG, and pET30yjjGEcpsuG, respectively. *KspsuG* (from *K. spallanzanii*), *RspsuG* (from *Rhizobium* sp. CF142), *SspsuG* (from *S. spinosa*), and *SppsuG* (from *S. platensis*) were cloned into pET30yjjGEcpsuG, digested with *Kpn*I and XhoI, yielding plasmids pET30yjjGKspsuG, pET30yjjGRspsuG, pET30yjjGSspsuG, and pET30yjjGSspsuG, respectively. All heterologous genes were synthesized by GenScript Bio Inc. (Nanjing, China), and the codons of the heterologous genes were optimized based on *E. coli* with GenSmart codon optimization performed by GenScript Bio. The sequences of the codon-optimized genes are presented in Table S5.

Construction of Recombinant Strains. The CRISPR-Cas9 system was applied to knock out genes in *E. coli* following methods described in a previous study.[29] Herein, the process used for the deletion of the *pepA* gene in *E. coli* MG1665 is described as an example of the method used. A gRNA plasmid from plasmid pTargetF was amplified by PCR using primers pepA20F/pepA20R, and the PCR products were transformed into competent *E. coli* DH5α cells after DpnI digestion. The two homologous arms (approximately 500 bp) from *E. coli* MG1655 were amplified by PCR using the primers pepA-F1/pepA-R1 and pepA-F2/pepA-R2. The full-length DNA fragment for homologous recombination was obtained by overlapping PCR products using primers pepA-F1 and pepA-R2. A single colony of MG1665 containing the plasmid pCAS9 was cultivated overnight in LB medium at 30 °C. Then, the cultures were transferred to fresh LB medium at a 2% inoculum volume, and arabinose was added to the culture to a final concentration of 10 mM. When the OD_{600} reached 0.6,

https://doi.org/10.1021/acsomega.3c05219
ACS Omega 2023, 8, 36386−36392

the cells were collected to prepare electrocompetent cells after washing twice with precooled 10% (v/v) glycerol. The gRNA plasmid and homologous DNA fragment were added into an electroshock cup to be transformed into competent cells through electroporation (1 mm cuvette, 1.8 kV). After electroporation, 1 mL of LB was immediately added, and the cells were allowed to recover at 30 °C for 1 h prior to plating on LB agar supplemented with ampicillin and spectinomycin. After 20 h, single transformants were verified by colony PCR using the primers pepVerF and pepVerR. The correct mutant strain was inoculated into 3 mL of LB medium cultured at 30 °C, and IPTG was added to the medium at a final concentration of 0.1 mM to cure the pTargetF derivative. The colonies cured in the pTarget series were used in the next round of gene knockout. The other mutant strains were constructed using a similar method.

Protein Expression, Purification, and SDS−PAGE Analysis. BL21(DE3) harboring overexpression plasmids were cultured overnight in LB medium containing 50 mg/L kanamycin at 37 °C. Then, the cultures were transferred to 30 mL of LB medium containing 50 mg/L kanamycin and grown at 37 °C until the OD_{600} reached 0.6−0.8. IPTG was subsequently added to a final concentration of 0.2 mM and incubated for 20 h at 25 °C. The culture was centrifuged at 4000 rpm and 4 °C for 5 min. The resulting pellet was resuspended in lysis buffer (20 mM phosphate buffer pH 8.0, 300 mM NaCl, 10 mM imidazole). The cells were lysed with a sonicator for a total of 10 min (3 s pulses and 6 s breaks). After sonication, the lysis solution was centrifuged at 15,000 rpm and 4 °C for 20 min. The supernatant was purified with a Ni-NTA column. The supernatant and loading buffer were boiled for 5 min, and then 10 μL of the mixture was loaded for sodium dodecyl sulfate−polyacrylamide gel electrophoresis (SDS−PAGE) (12% polyacrylamide gel) analysis.

Enzymatic Assays of Phosphatase and ΨMP Glycosidase. The phosphatase catalytic reaction was performed in 20 mM phosphate buffer (pH 7.0), 10.0 mM $MgCl_2$, 1.0 μM phosphatase, and 0.5−10 mM pseudouridine 5′-monophosphate. Reactions were performed on a 100 μL scale and incubated at 30 °C. The ΨMP glycosidase catalytic reaction was performed in 20 mM phosphate buffer (pH 7.0) with 100 mM ribose 5-phosphate, 0.5−10 mM uracil, 1.0 mM $MnCl_2$, and 1.0 μM ΨMP glycosidase. The reactions were performed on a 100 μL scale and incubated at 30 °C. The kinetic parameters (K_m and k_{cat}) were measured with substrate concentrations between 0.5 and 10 mM and calculated according to the Michaelis−Menten plot.

Analytical Methods. The concentration of pseudouridine was measured by high-performance liquid chromatography (Agilent 1260 Series) equipped with a TC-C18 column (250 × 4.6 mm, Agilent) and monitored at a wavelength of 260 nm. The column was operated at 30 °C with a mobile phase consisting of 0.2% ammonium acetate and acetonitrile (95:5, v/v) at a flow rate of 1.0 mL/min.

Ψ Isolation. The fermentation broth was centrifuged (6000*g*, 5 min) to obtain the supernatant, and the supernatant was freeze-dried. The crude pseudouridine was purified by semipreparative HPLC (Agilent 1260, Zorbax SB-C18, 5 μm, 250 × 9.4 mm inner diameter; 1.5 mL/min; 260 nm) using a solvent of CH_3CN/H_2O (5:95, v/v) to give Ψ. The product (purity >95%) was analyzed by MS and NMR.

■ ASSOCIATED CONTENT

Supporting Information

The Supporting Information is available free of charge at https://pubs.acs.org/doi/10.1021/acsomega.3c05219.

Mass spectrum of pseudouridine isolated from the fermentation broth of *E. coli*; ^1H NMR spectra of pseudouridine isolated from the fermentation broth of *E. coli*; ^{13}C NMR spectra of pseudouridine isolated from the fermentation broth of *E. coli*; HPLC analysis of fermentation broth of *E. coli*; SDS−PAGE analysis of the supernatant of phosphatase genes overexpressed in *E. coli*; evolutionary tree of PsuG proteins; SDS−PAGE analyses of the supernatant of *psuG* genes overexpressed in *E. coli*; kinetic parameters of phosphatase; kinetic parameters of ΨMP glycosidase; bacterial strains and plasmids used in this study; primers used for plasmid construction and gene knockout; and the sequences of codon-optimized genes (PDF)

■ AUTHOR INFORMATION

Corresponding Author

Min Zhou − *Institute of Biopharmaceuticals, School of Pharmaceutical Sciences, Taizhou University, Taizhou 318000, China;* orcid.org/0009-0007-2312-1867; Email: zhoumin@tzc.edu.cn

Authors

Ruyu Tang − *Institute of Biopharmaceuticals, School of Pharmaceutical Sciences, Taizhou University, Taizhou 318000, China*

Liyuan Wei − *Institute of Biopharmaceuticals, School of Pharmaceutical Sciences, Taizhou University, Taizhou 318000, China*

Jidong Wang − *Key Laboratory of Vector Biology and Pathogen Control of Zhejiang Province, College of Life Science, Huzhou University, Huzhou 313000, China*

Huan Qi − *Key Laboratory of Vector Biology and Pathogen Control of Zhejiang Province, College of Life Science, Huzhou University, Huzhou 313000, China*

Complete contact information is available at: https://pubs.acs.org/10.1021/acsomega.3c05219

Author Contributions

M.Z. conceived and structured the work, conducted fermentation experiments in bioreactors, and wrote the manuscript. R.T. constructed plasmids and strains. L.W. conducted protein overexpression experiments and fermentation experiments in shake flasks. J.W.,and H.Q performed compound isolation, purification, and analysis.

Notes

The authors declare no competing financial interest.

■ ACKNOWLEDGMENTS

This work was supported by scientific research start-up funding from Taizhou University (T20200201031). The authors acknowledge the excellent suggestions provided by Prof. Yongquan Li and Xuming Mao (Zhejiang University).

■ ABBREVIATIONS

Ψ, pseudouridine; ΨMP, pseudouridine-5′-phosphate glycosidase; *psuG*, encoding gene of pseudouridine 5′-phosphate

glycosidase; *KspsuG*, psuG gene from *Klebsiella spallanzanii*; *RspsuG*, psuG gene from *Rhizobium* sp. CF142; *SspsuG*, psuG gene from *Saccharopolyspora spinosa*; *SppsuGx*, psuG gene from *Streptomyces platensis*

REFERENCES

(1) Davis, F. F.; Allen, F. W. Ribonucleic acids from yeast which contain a fifth nucleotide. *J. Biol. Chem.* **1957**, *227*, 907−915.

(2) Schwartz, S.; Bernstein, D.; Mumbach, M.; Jovanovic, M.; Herbst, R.; León-Ricardo, B.; Engreitz, J.; Guttman, M.; Satija, R.; Lander, E.; Fink, G.; Regev, A. Transcriptome-wide mapping reveals widespread dynamic-regulated pseudouridylation of ncRNA and mRNA. *Cell* **2014**, *159*, 148−162.

(3) Ge, J. H.; Yu, Y. T. RNA pseudouridylation: new insights into an old modification. *Trends Biochem. Sci.* **2013**, *38*, 210−218.

(4) Davis, D. R. Stabilization of RNA stacking by pseudouridine. *Nucleic Acids Res.* **1995**, *23*, 5020−5026.

(5) Andries, O.; Mc Cafferty, S.; De Smedt, S. C.; Weiss, R.; Sanders, N.; Kitada, T. N1-methylpseudouridine-incorporated mRNA outperforms pseudouridine incorporated mRNA by providing enhanced protein expression and reduced immunogenicity in mammalian cell lines and mice. *J. Controlled Release* **2015**, *217*, 337−344.

(6) Anderson, B. R.; Muramatsu, H.; Nallagatla, S. R.; Bevilacqua, P. C.; Sansing, L. H.; Weissman, D.; Karikó, K. Incorporation of pseudouridine into mRNA enhances translation by diminishing PKR activation. *Nucleic Acids Res.* **2010**, *38*, 5884−5892.

(7) Morais, P.; Adachi, H.; Yu, Y. T. The Critical Contribution of Pseudouridine to mRNA COVID-19 Vaccines. *Front. Cell Dev. Biol.* **2021**, *9*, 789427.

(8) The Clinical Trials Database. 2000. https://www.clinicaltrials.gov (accessed Feb 29, 2000).

(9) Shapiro, R.; Chambers, R. SYNTHESIS OF PSEUDOURIDINE. *J. Am. Chem. Soc.* **1961**, *83*, 3920−3921.

(10) Yu, C. P.; Chang, H. Y.; Chien, T. C. Total synthesis of pseudouridine via Heck-type C-glycosylation. *New J. Chem.* **2019**, *43*, 8796−8803.

(11) Koonin, E. V. Pseudouridine synthases: four families of enzymes containing a putative uridine-binding motif also conserved in dUTPases and dCTP deaminases. *Nucleic Acids Res.* **1996**, *24*, 2411−2415.

(12) Conrad, J.; Sun, D.; Englund, N.; Ofengand, J. The rluC Gene of Escherichia coli Codes for a Pseudouridine Synthase That Is Solely Responsible for Synthesis of Pseudouridine at Positions 955, 2504, and 2580 in 23S Ribosomal RNA. *J. Biol. Chem.* **1998**, *273*, 18562−18566.

(13) Preumont, A.; Snoussi, K.; Stroobant, V.; Collet, J. F.; Van Schaftingen, E. Molecular Identification of Pseudouridine-metabolizing Enzymes. *J. Biol. Chem.* **2008**, *283*, 25238−25246.

(14) Pfeiffer, M.; Ribar, A.; Nidetzky, B. A selective and atom-economic rearrangement of uridine by cascade biocatalysis for production of pseudouridine. *Nat. Commun.* **2023**, *14*, 2261.

(15) Riley, A. T.; Sanford, T. C.; Woodard, A. M.; Clerc, E. P.; Sumita, M. Semi-enzymatic synthesis of pseudouridine. *Bioorg. Med. Chem. Lett.* **2021**, *44*, 128105.

(16) Yang, D.; Park, S. Y.; Park, Y. S.; Eun, H.; Lee, S. Y. Metabolic Engineering of Escherichia coli for Natural Product Biosynthesis. *Trends Biotechnol.* **2020**, *38*, 745−765.

(17) Wu, H.; Li, Y.; Ma, Q.; Li, Q.; Jia, Z. F.; Yang, B.; Xu, Q. Y.; Fan, X. G.; Zhang, C. L.; Chen, N.; Xie, X. X. Metabolic engineering of Escherichia coli for high-yield uridine production. *Metab. Eng.* **2018**, *49*, 248−256.

(18) Yang, K.; Li, Z. M. Multistep construction of metabolically engineered Escherichia coli for enhanced cytidine biosynthesis. *Biochem. Eng. J.* **2020**, *154*, 107433.

(19) Asahi, S.; Tsunemi, Y.; Doi, M. Effects of homoserine dehydrogenase defificiency on production of cytidine by mutants Bacillus subtilis. *Biosci. Biotechnol. Biochem.* **1996**, *60*, 353−354.

(20) Koo, B. S.; Hyun, H. H.; Kim, S. Y.; Kim, C. H.; Lee, H. C. Enhancement of thymidine production in E. coli by eliminating repressors regulating the carbamoyl phosphate synthetase operon. *Biotechnol. Lett.* **2011**, *33*, 71−78.

(21) Pfeiffer, M.; Nidetzky, B. Reverse C-glycosidase reaction provides C-nucleotide building blocks of xenobiotic nucleic acids. *Nat. Commun.* **2020**, *11*, 6270.

(22) Kuznetsova, E.; Nocek, B.; Brown, G.; Makarova, K. S.; Flick, R.; Wolf, Y. I.; Khusnutdinova, A.; Evdokimova, E.; Jin, K.; Tan, K. M.; Hanson, A. D.; Hasnain, G.; Zallot, R.; de Crécy-Lagard, V.; Babu, M.; Savchenko, A.; Joachimiak, A.; Edwards, A. M.; Koonin, E. V.; Yakunin, A. F. Functional Diversity of Haloacid Dehalogenase Superfamily Phosphatases from Saccharomyces cerevisiae. *Arch. Biochem. Biophys.* **2015**, *290*, 18678−18698.

(23) Sosio, M.; Gaspari, E.; Iorio, M.; Pessina, S.; Medema, M. H.; Bernasconi, A.; Simone, M.; Maffioli, S. I.; Ebright, R. H.; Donadio, S. Analysis of the Pseudouridimycin Biosynthetic Pathway Provides Insights into the Formation of C-nucleoside Antibiotics. *Cell Chem. Biol.* **2018**, *25*, 540.

(24) Thapa, K.; Oja, T.; Metsä-Ketelä, M. Molecular evolution of the bacterial pseudouridine-5′-phosphate glycosidase protein family. *FEBS J.* **2014**, *281*, 4439−4449.

(25) Argoudelis, A. D.; Mizsak, S. A. 1-methylpseudouridine, a metabolite of Streptomyces platensis. *J. Antibiot.* **1976**, *29*, 818−823.

(26) Feng, J.; Li, C. Q.; He, H.; Xu, S.; Wang, X.; Chen, K. Q. Construction of cell factory through combinatorial metabolic engineering for efficient production of itaconic acid. *Microb. Cell Factories* **2022**, *21*, 275.

(27) Huang, Z. S.; Li, N.; Yu, S. Q.; Zhang, W. P.; Zhang, T. M.; Zhou, J. W. Systematic Engineeringof Escherichia coli for Efficient Production of Nicotinamide Mononucleotide From Nicotinamide. *ACS Synth. Biol.* **2022**, *11*, 2979−2988.

(28) Karp, P. D.; Billington, R.; Caspi, R.; Fulcher, C. A.; Latendresse, M.; Kothari, A.; Keseler, I. M.; Krummenacker, M.; Midford, P. E.; Ong, Q.; Ong, W. K.; Paley, S. M.; Subhraveti, P. The BioCyc collection of microbial genomes and metabolic pathways. *Briefings Bioinf.* **2019**, *20*, 1085−1093.

(29) Jiang, Y.; Chen, B.; Duan, C. L.; Sun, B. B.; Yang, J. J.; Yang, S. Multigene editing in the Escherichia coli genome via the CRISPR-Cas9 system. *Appl. Environ. Microbiol.* **2015**, *81*, 2506−2514.

https://doi.org/10.1021/acsomega.3c05219
ACS Omega 2023, 8, 36386−36392